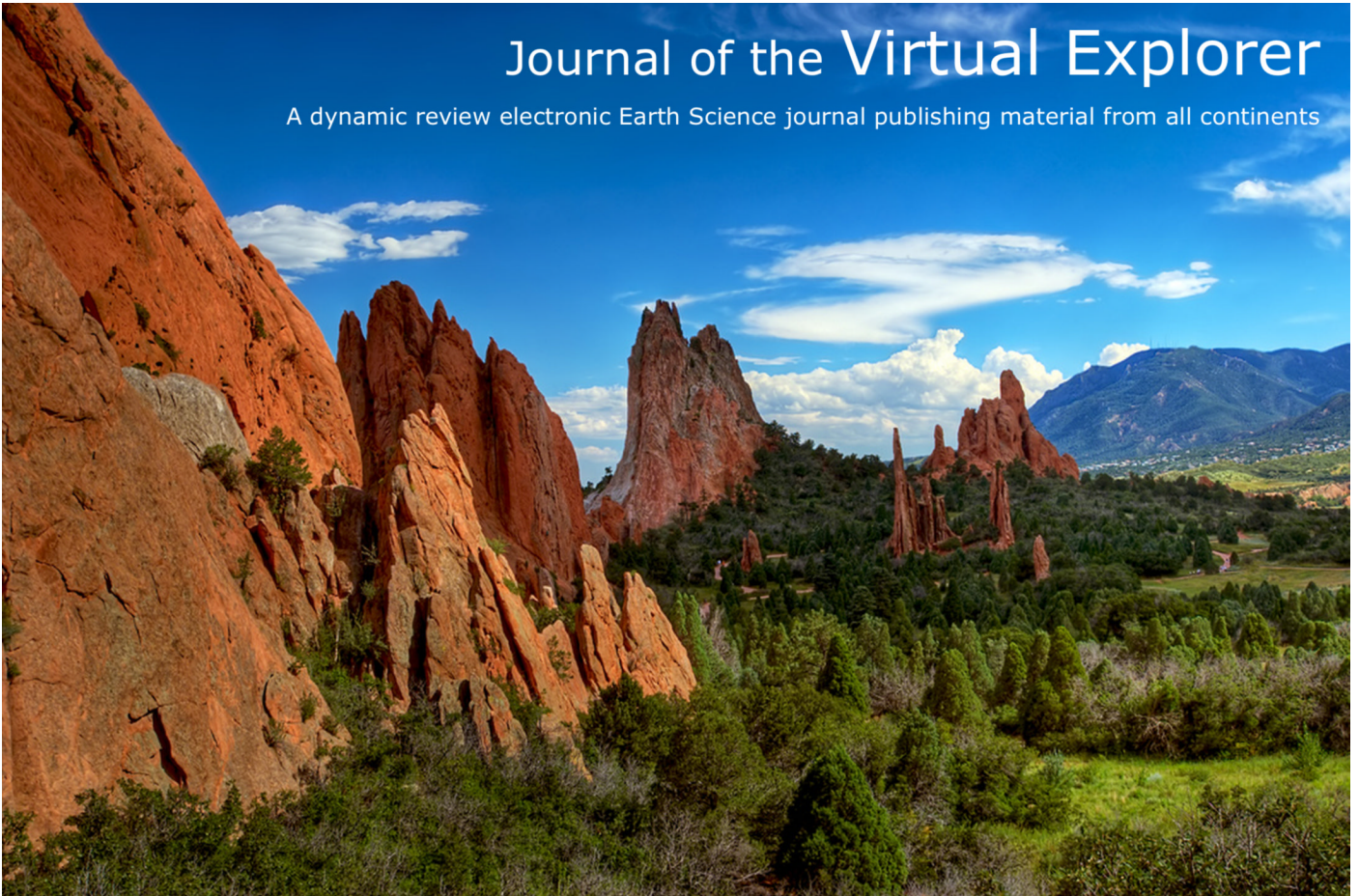


Journal of the Virtual Explorer

A dynamic review electronic Earth Science journal publishing material from all continents



Some Frequently Asked Questions about the Mount Isa Deposit, and Enigmatic Textures of the Ores

W.G. Perkins

Journal of the Virtual Explorer, Electronic Edition, ISSN 1441-8142, volume 28, paper 1
In: (Eds.) Gideon Rosenbaum, Declan De Paor, Daniel Köhn, Guiting Hou, and Talat Ahmad, General Contributions, 2008.

Download from: <http://virtualexplorer.com.au/article/2008/187/faqs-about-the-mt-isa-deposit>

Click <http://virtualexplorer.com.au/subscribe/> to subscribe to the Journal of the Virtual Explorer.
Email team@virtualexplorer.com.au to contact a member of the Virtual Explorer team.

Copyright is shared by The Virtual Explorer Pty Ltd with authors of individual contributions. Individual authors may use a single figure and/or a table and/or a brief paragraph or two of text in a subsequent work, provided this work is of a scientific nature, and intended for use in a learned journal, book or other peer reviewed publication. Copies of this article may be made in unlimited numbers for use in a classroom, to further education and science. The Virtual Explorer Pty Ltd is a scientific publisher and intends that appropriate professional standards be met in any of its publications.



Some Frequently Asked Questions about the Mount Isa Deposit, and Enigmatic Textures of the Ores

W.G. Perkins

Journal of the Virtual Explorer, Electronic Edition, ISSN 1441-8142, volume **28**, paper 1
In: (Eds.) Gideon Rosenbaum, Declan De Paor, Daniel Köhn, Guiting Hou, and Talat Ahmad,
General Contributions, 2008.

Abstract: There is ongoing debate about the relative and absolute timing of formation of the Mount Isa copper and lead-zinc orebodies. This paper provides additional examples to support those illustrated in Perkins (1997,1998) and Perkins *et al.* (1998), which argued that these ore systems were cogenetic and formed late in the main deformation event which affected the mine environment (D₃). This is done in terms of key questions which are often asked about the deposit, particularly in a regional context.

<http://virtualexplorer.com.au/article/2008/187/faqs-about-the-mt-isa-deposit>

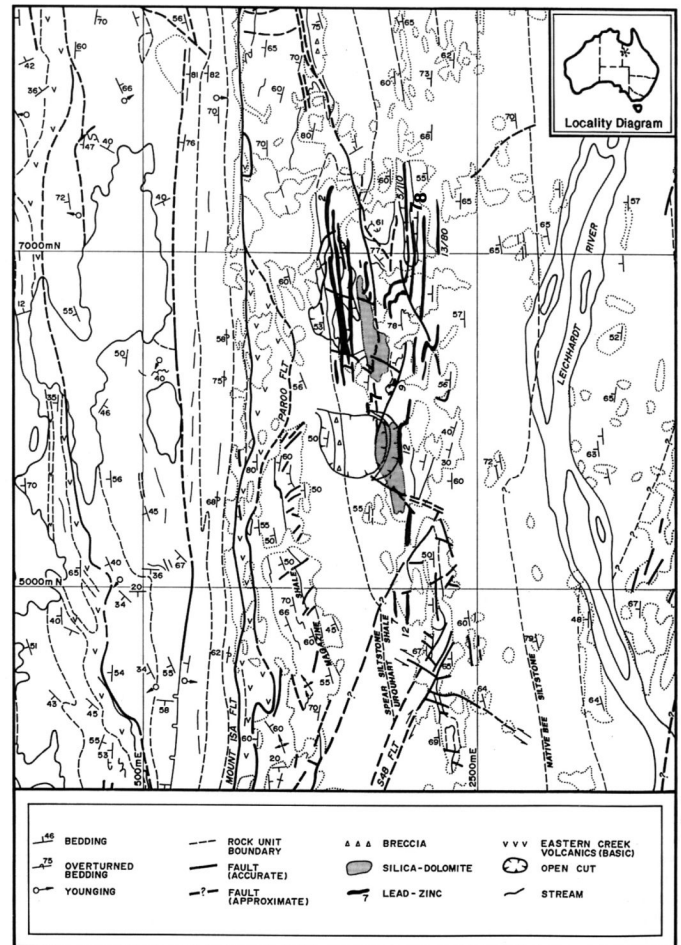
Citation: Perkins, W. 2008. Some Frequently Asked Questions about the Mount Isa Deposit, and Enigmatic Textures of the Ores. In: (Eds.) Gideon Rosenbaum, Declan De Paor, Daniel Köhn, Guiting Hou, and Talat Ahmad, *Journal of the Virtual Explorer*, volume **28**, paper 1, doi: 10.3809/jvirtex.2008.00187

Introduction

This paper results from questions provoked by geologists involved with the Mount Isa deposits and discussions pursued over the last year, particularly on observation of rock exposures and drill core. The most debated issue remains the timing relationship between the lead-zinc and copper deposits at Mount Isa itself. Also addressed are questions raised by Painter *et al.* (1999), particularly with respect to the timing of fine-grained pyrite formation. As this paper was being revised following reviewers' comments, another paper (Davis, 2004) was published. It adds considerable data on geometry and metal distribution on the lead-zinc orebodies and concludes that the lead-zinc orebodies were structurally controlled during D₄ which corresponds with D₃ of this paper. It is not discussed further here.

The questions are ordered with respect to those which relate to the orebody environment, the copper orebodies and the lead-zinc orebodies. An overview of the mine area is shown in Figure 1, which illustrates the relative positions of the lead-zinc and copper orebodies (highlighting those referred to in the text) and their relationship to the Paroo-Baseament fault.

Figure 1. Surface map of the mine area.



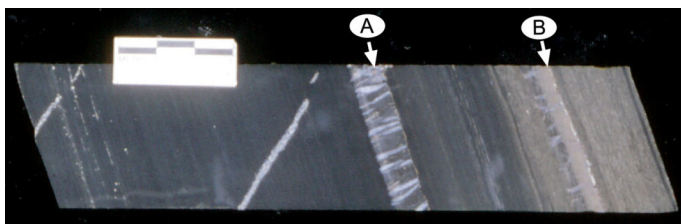
Surface map of the mine area showing the main geological features and the relationship of the ore environment to the major structures. Only the basic volcanic sequences of the Eastern Creek Volcanics have been highlighted (rock symbol v). East of the Paroo Fault are formations of the Mount Isa Group. Lead-zinc orebodies (with identifying numbers) in the Urquhart Shale have been projected from the closest data in unweathered rock to show an estimate of original ore at the current erosion level. Orebodies 7 and 8 mentioned in the text have been shown in bolder numerals. Silica-dolomite is from the 1966 surface mapping by W.D Smith (pers. comm. 1994), updated by more recent drilling (S. de Kruijff, pers. comm., 1983). The unconformity west of the Mount Isa fault was mapped by J.M. Proffett in 1989 (Proffett, 1990). Modified from 1:2500 map compiled by P. Stoker, 1991. Outcrop boundaries are not shown west of the Mount Isa Fault, which is generally an area of good exposures. Inset. Location of Mount Isa.

FAQ-1. What is the nature of the "tuff marker beds"?

Distinctive layers within the mine sequence have been used for correlation of orebodies from the earliest mine

mapping, where they were called "cross fracture beds (XFB's)", referring to their tendency to form overprinting fractures and veins in their cherty basal portions, Figure 2, (Perkins, 1984, fig. 4). Two alternative origins have been proposed: a volcanoclastic origin, and evaporite brines altering a pre-existing sediment.

Figure 2. Marker beds of the "B" sequence.



Feldspathic marker bed (A) in drill core. Highly veined grey cherty layer. B is also a marker bed but is here obscured by sphalerite. No. 7 orebody B sequence. Locality unknown.

Croxford (1964) studied No 7 lead-zinc orebody at 6775mN on 8 Level. At this location the hangingwall marker beds (defined "A" sequence described in Perkins (1984) and "B" sequence of Perkins (1997), were obliterated by silica-dolomite, but the main (~60mm) footwall marker was well developed. Croxford studied this marker and many others throughout the mine, as well as similar layers in the district. The most important observation was of textures identified as glass shards indicating a volcanic origin. These textures were highlighted by dusty rutile along selected grain boundaries of microcrystalline potash feldspar. Other observations showed the shard outlines in a groundmass of galena (Croxford, pers. comm. 1994). Further work on the composition of these layers showed them to be highly potassic, commonly containing up to 85% microcline. Croxford found this to be an unlikely original volcanic composition, but suggested that features such as embayed quartz crystal fragments and the absence of ferromagnesian minerals indicated possible rhyolitic affinities of the parent magma. He concluded that the volcanic glass "underwent post-depositional changes in order to adopt the most stable chemical and physical configuration, -in this case a low-temperature orthoclase as indicated by the low soda content". Since Croxford's work the layers have been referred to as "tuff marker beds (TMB's)".

Although Croxford considered the possibility that a "hydrothermal concept of ore genesis for the lead-zinc ores might equate potash enrichment with hydrothermal

mineralization", he preferred the interpretation that the volcanic glass of the cross-fracture beds derived their potassium from connate water. Noting that individual beds (other than the cross-fracture beds) also contained up to 8% potash, that potash feldspar was a dominant component of the mineralized sequence, and that "pellets" in some thin beds exhibited the same textures as the cross-fracture beds, Croxford concluded that the entire sequence was "to a large degree composed of potash-enriched volcanic material". The amount of potash in the gradational tops of the markers and the overlying sequences was regarded as a proxy for the original proportion of tuffaceous material in the sediments. It became routine in mine logging to stain suspected markers, with the intensity of yellow stain indicating the proportion of potash.

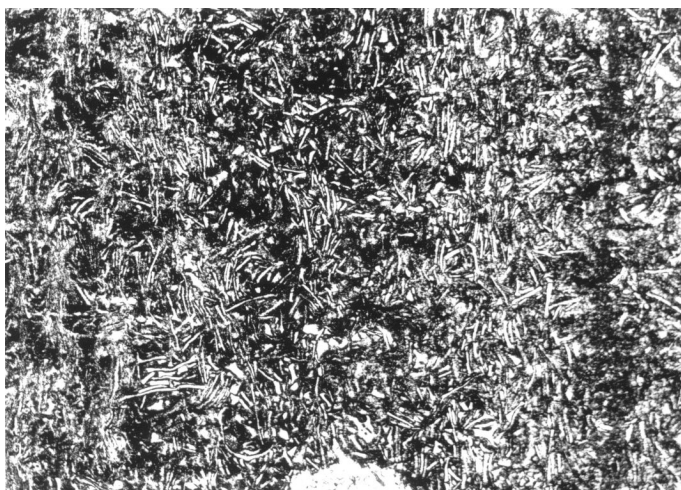
A volcanic origin for the Urquhart Shale was challenged by Neudert (1983) who recognized detrital K-feldspar and as overgrowths on grains, as well as the "pellets" described by Croxford and chert in the cross-fracture beds. Neudert found cherty K-feldspar to be most abundant in the Urquhart Shale, but to also occur in other parts of the Upper Mount Isa Group. He regarded the "pellet" forms as detrital in appearance and, in the mineralized zones of facies I, they were intergrown with other rock components and "often represent a major rock component" P. 142. Lath forms were replaced by K-feldspar; calcite poikilotopes enclosed remnants of the dolomite-K-feldspar matrix and were surrounded by cherty K-feldspar. Neudert used these lines of evidence to indicate that evaporite brines were the source of the alkalis for the formation of authigenic feldspars. He disagreed (p167) with Croxford (1964) that K-feldspar had formed exclusively by volume-for-volume replacement of volcanic material, listing other forms which were not volcanic, and noting that not only the shards consisted of detrital K-feldspar but also the interstitial areas.

According to Paterson, D. J., (pers comm 2003) only about 10% of the marker beds contain recognizable shard textures. In this author's study of the lead-zinc orebodies (Perkins, 1997), the two markers bounding the 7 O/B "B" sequence (12 localities) and the footwall marker (5 localities), have been examined in thin section. In only the most distal locality (41000mN. Perkins, 1997, p.74) are shard textures recognized in these three markers. The footwall marker (30mm thick) contains the best-preserved shards (Figure 3) in the basal 3mm. The bed shows slight lamination suggesting very minor

reworking. There is minimal dissolution indicating little shortening normal to bedding. It appears to be largely an air fall tephra. The central part of the marker consists of an interlocking mass of sericite. The same bed elsewhere is highly biotitic along strike from where it is a feldspathic chert (Perkins, 1997 p.74).

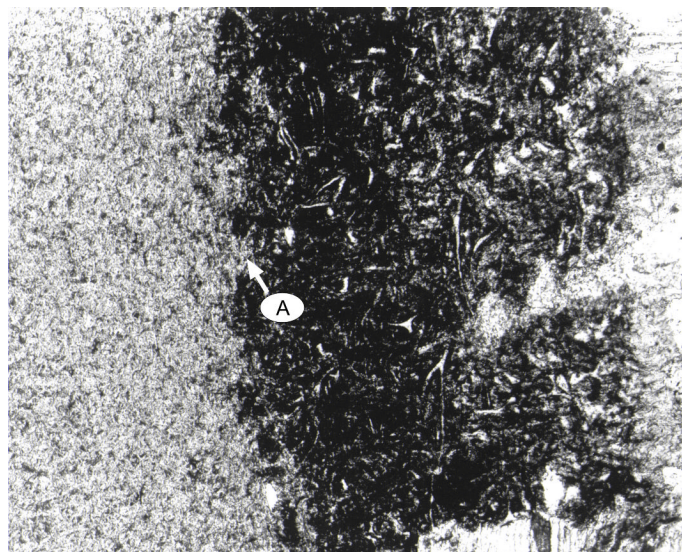
In the marker at the top of the "B" sequence only ~0.8 mm at the base contains well preserved shards in a carbonaceous groundmass. The remaining 5mm is a fine intergrowth of sericite (Figure 4). Boundary textures with the gradual disappearance of shard outlines into the sericitic area indicate sericitic alteration. These textures indicate that volcanoclastic textures are only locally preserved, within what are unequivocally correlatable layers, and that the feldspars and micas are alteration products.

Figure 3. TMB with shard textures.



Close-packed shard textures in a carbonaceous groundmass. Bedding is parallel to the short side of the photograph. Younging unknown. 7 O/B F/W TMB DDH QZ10 1039.38m. Field of view 1.7mm.

Figure 4. Micaceous alteration in a TMB.



Shard textures in carbonaceous groundmass. Younging is to left of the photograph. The lower grey area (on the right) is a dolomite vein system and there is a gradational boundary (eg. at A) into fine sericite, indicating micaceous alteration. 7 O/B "B"sequence TMB QZ10 1034.85m. Field of view 1.7mm.

Neudert (1983) noted a direct textural association of authigenic feldspars (albite as well as K-feldspar) with metasomatic carbonate and canvassed the model of a hydrothermal origin for these minerals. He envisaged hydrothermal introduction from basin margin faults at stages from within the first few centimeters of sediment to late diagenesis but prior to final induration. Because of its zonal pattern consistent with other alteration features associated with lead-zinc mineralization, such as bleaching and "buff alteration", pyrrhotite deposition and iron-rich zones, Perkins (1997) argued that the cherty K-feldspar in the TMB's represented an early stage of hydrothermal alteration zoned around the deformed fault contact between the Urquhart shale and altered Eastern Creek Volcanics.

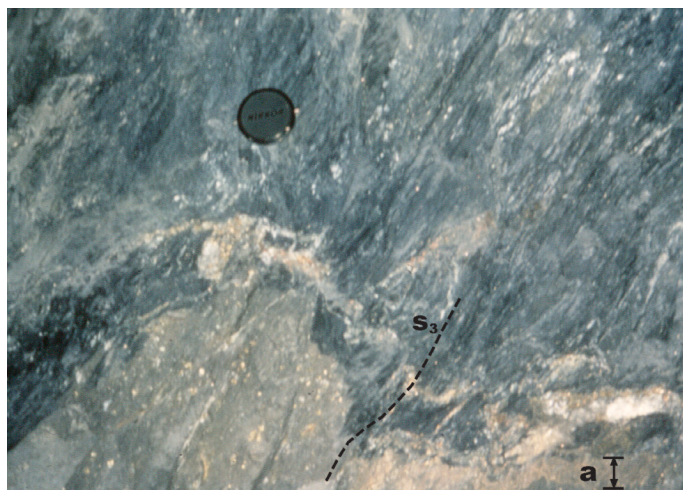
Neudert (1983) p.195 argued that his "feldspathic cherts" which did not contain recognizable shards could either be volcanic ash, deposits from turbulent suspension currents, or evaporites, and preferred that the generic term "tuffaceous marker beds" should not be used. From Perkins (1997), it is recommended that the distinctive and persistent cherty markers used by Mine geologists for correlation continue to be called TMB's. However, this author agrees with Neudert (1983) that the presence of

authigenic K-feldspar does not signify a volcanic sequence, but is an alteration product, albeit much younger than that envisaged by Neudert.

FAQ- 2. What is the nature of the Paroo/ Basement fault in the Mine?

At issue is whether this fault is a late post-Cu ore structure or whether it is an earlier structure which is affected by deformation at the mine scale. A further issue is whether it formed as a normal or reverse fault. At many localities on the surface this fault contact between altered Eastern Creek Volcanics and the Mount Isa Group is not well exposed. Proffett (1990) recognised this fault along the northern margin of the Crystallina Block and showed it to be overprinted by the north-south cleavage. This contact had earlier been mapped as a younger fault. Folded exposures of the fault separating deformed Urquhart Shale from chlorite schists at deep levels in the Mine are shown in Perkins (1984). Figure 5 shows this shear zone strongly altered by rutile, which is folded and overprinted by a strong west-dipping foliation (S_3). Figure 6 illustrates the same healed contact further south where it is cut and displaced by the Buck Quartz Fault.

Figure 5. Folded Paroo-Basement Fault beneath the 1100 orebody.



Exposure of the Paroo-Basement Fault beneath the northern part of the 1100 orebody. A 50mm yellow-green rutile-altered shear zone (eg at a) is within strongly altered basic volcanics and against carbonaceous slates of the Urquhart Shale. It has been folded and overprinted by the S_3 cleavage. 17C sublevel 5400mN.

Figure 6. Paroo-Basement Fault cut by the Buck Quartz Fault.



Healed contact between chlorite schists of the Eastern Creek Volcanics and carbonaceous slates of the Breakaway Shale. There are blocks of schist extending upwards into the slate-rich shear zone. This early fault a is cut by the Buck Quartz Fault (b) consisting of quartz veins and carbonaceous mylonite. Photo courtesy D. Sims. 19C sublevel 4010N Looking North.

These illustrations show that the nature of the complex contact zone beneath the copper orebodies depend on whether it is observed further northwards where the contact is as shown in Figure 5 or southwards where it appears as the quartz-mylonite zone (referred to as the Buck Quartz Fault) Figure 6. Whether the folded contact is a normal or reverse fault remains equivocal. All criteria show the Buck Quartz Fault to be a reverse fault which cuts and displaces the Paroo-Basement Fault.

FAQ- 3. Do the mineral assemblages of successive vein generations reflect the fluid compositions at different stages?

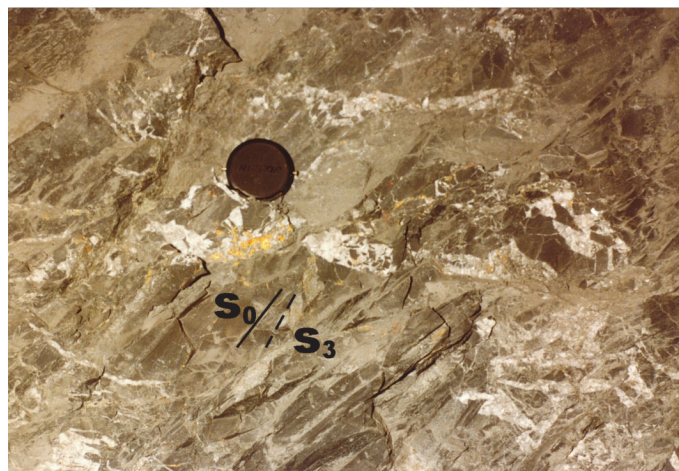
Determination of a fluid evolution history for the copper orebodies is, to a large extent, influenced by interpretation of overprinting criteria in the alteration system (Heinrich *et al.*, 1989, Waring, 1990). Of most interest are the depositional conditions and fluids responsible for the economic sulphides. Perkins (1984) and Swager (1985) illustrated and described a sequencing of dolomite and quartz veins and breccias, all of which contained sulphides, principally chalcopyrite. Analysis of veins from epigenetic deposits generally assumes that the veins are essentially dilational, and consequently that all minerals were deposited within each vein generation prior to the subsequent generation. In these scenarios the evolving

fluid composition must be capable of depositing the observed sulphides in the overprinting veins. Such an argument has been applied to Mount Isa copper genesis by J. M. Proffett (internal report to MIM Exploration-1992), that since chalcopyrite is observed in veins which have been deformed during the mine folding (D_3 of Perkins 1984 and Main Slaty Cleavage event of Proffett 1992), then this represents the timing of the bulk of the copper orebodies. Chalcopyrite in still younger veins is thus the result of "remobilization" or a younger generation deposited with the components of that vein. An alternative interpretation where the sulphides are not deposited in any of the veins until the youngest veins have formed, changes the notion of timing of the orebody and implies an evolving fluid history consistent with that late deposition.

Significance of Replacement Veining

A key factor in the mineral deposition evolution is the question of whether the dolomite-silica-sulphide breccia systems are predominantly dilational or replacive. Arguments that dolomitic breccia systems develop from veins which are predominantly replacive rather than dilational, are advanced in Perkins (1984) see example Figure 7. Notwithstanding relatively sharp vein and breccia fragment boundaries, detailed examination shows that vein walls and breccia fragments cannot be fitted together, by movement along bedding and/or cleavage. Even though there has been some movement of fragments the net result is a pseudobreccia resulting from wall rock replacement by coarse-grained dolomite during deformation. Vein systems contain successive generations of dolomite, the earliest of which show deformation twinning. Chalcopyrite exhibits replacive growth across the boundaries of these dolomites, similar to the galena/sphalerite relationship illustrated in Perkins (1997, fig 15e) and shows no evidence of being deformed or of subsequent dissolution.

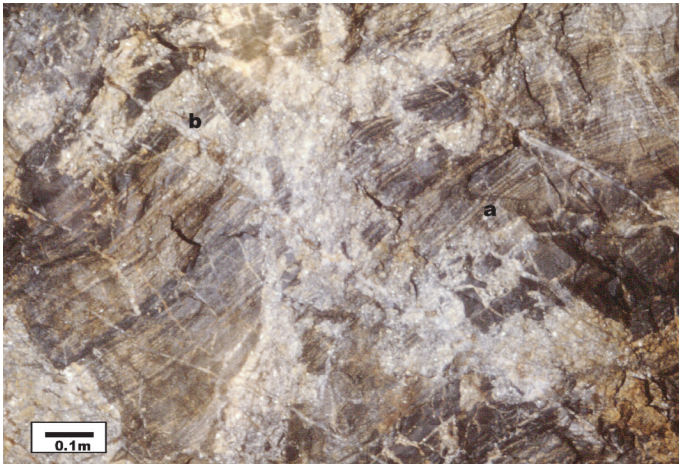
Figure 7. Shallow east-dipping vein and breccia systems in a dolomitic slate.



Dolomitic slate showing nature of breccia vein system. Even though fragment and vein margins are quite sharp, many of the breccias are "blind", the fragments are almost in situ and cannot be fitted together by movement along bedding (S_0) and/or cleavage (S_3). This shows that wall rock replacement is the dominant process in vein and breccia formation. Replacement of the coarse-grained dolomite by chalcopyrite is quite variable. 18E Sublevel. 4576mN, 1908mE. Looking north.

The youngest veins in the copper orebodies dip at 25° - 35° east (Figure 8), and commonly contain mostly quartz, even where the earlier veins and breccias are dolomitic. Using the arguments developed in Perkins (1984, 1997) indicating that quartz in the orebody zones is pseudomorphic after dolomite, this suggests that veins of this orientation were preferentially silicified. The stronger association of chalcopyrite with quartz explains why these veins are the most chalcopyrite-rich in the outer dolomitic parts of the "silica-dolomite". Even where cross-cutting dolomite alteration lobes are totally replaced by silica (Figure 9), the shallow east-dipping veins are commonly visible. The relationship of shallow-dipping veins to Mine folding (D_3) is illustrated in Figure 10 and Figure 11. These veins are superimposed on an open syncline and a breccia-imposed fault. Chalcopyrite masses have grown along, and over, these post-folding veins. Breccia textures in Figure 11 can be compared with those in Figure 8 with the difference being the deposition of quartz and chalcopyrite at the expense of dolomite. At this scale, as well as at the microscopic scale, there is no evidence of significant dilation associated with chalcopyrite deposition.

Figure 8. Breccia vein complex superimposed on a bedding-dolomitized sequence.



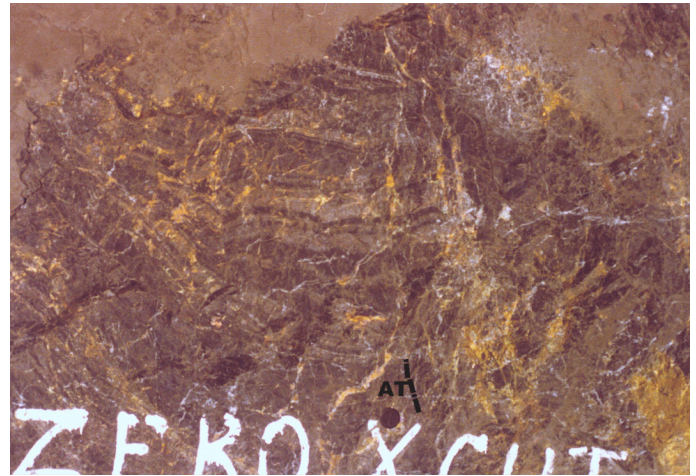
The gently folded bedding (major anticlinal hinge to the right) can be traced through the unrotated residual fragments. Many of the breccias terminate abruptly (eg. a) and are consistent with fracture-controlled replacement by dolomite rather than dilation. Gently east-dipping veins (eg. b) are mostly quartz but show dolomite residuals. Chalcopyrite is locally continuous across the vein boundary. 9 Level, 5415mN. Looking north.

Figure 9. Margin of silicified dolomite lobe.



Cross-cutting mottled grey zone of former dolomitic alteration (now totally silicified) showing vague outlines of gently east-dipping veins. The vein (a) above the lens cap is truncated to the right by a chalcopyrite-rich zone along relict bedding, dipping intermediate west. Shallow east-dipping veins in the silicified black non-laminated layer contain high proportions of chalcopyrite (b). 18E sublevel, 4345mN, 1972mE. Looking north.

Figure 10. Open D₃ fold with silicification and mineralization.



The axial trace (AT) of the D₃ syncline is shown. Sub-horizontal and shallow east-dipping veins continue across the fold irrespective of bedding orientation. 1100 orebody, 4500mN. Looking south.

Figure 11. Detail of Figure 10.



Sub-vertical breccia zone cutting across the fold and following the axial trace of the anticline. Matching of beds shows

a displacement across the zone of approximately 0.5m (right side up). The horizontal narrow quartz vein 100mm above "C" has not been displaced but is overprinted by chalcopyrite.

Implications for physico-chemical conditions of sulphide deposition

Deformation throughout the rock mass appears to have been essentially complete by the time of chalcopyrite (and also galena and sphalerite) deposition. Since textures at both meso and micro-scale show volume-for-volume replacement of gangue minerals by sulphides, geochemical models have to account for absolutely minimal porosity. Permeability appears to have been accommodated by dissolution of pre-existing phases by replacement, and fluid conditions must account for mass dissolution of these phases.

There is no evidence for successive generations of chalcopyrite deposition, indicating an evolving fluid which deposited sulphides as the final phase. Heinrich *et al.* (1989) supported the observations of Perkins (1984) that quartz deposition was pseudomorphic after dolomite, but used fluid inclusion and stable isotope data to argue against a model of simultaneously advancing fronts of dolomitization and silicification. They could not establish conditions under which the NaCl-rich brine responsible for deposition of quartz could have changed through the orebody environment to become the CaCl₂-rich fluid involved in the main phase of dolomite growth. It is difficult to determine conditions and fluids responsible for chalcopyrite, galena and sphalerite formation since associated non-sulphides were previously deposited, and conditions could have changed markedly since that stage. More work could potentially be done on fluid inclusions in sphalerite to give more controls on the mineralization stage.

FAQ- 4. How do the outer limits of lead-zinc orebodies fade out?

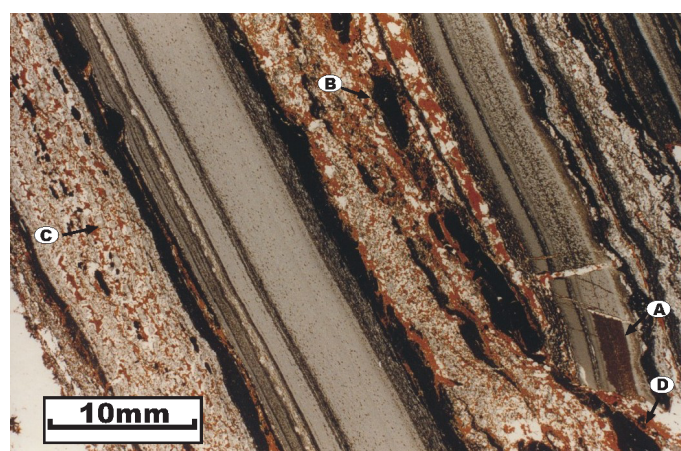
Some early work in studying the lead-zinc orebodies eg Croxford (1962) was hampered by the lack of mine development into the lateral extremities of the orebodies. This was rectified during the late 1980's with continued mining north of 7060mN. In particular, it allowed the investigation of lead-zinc orebodies as they approached the hinge of the Mount Isa Fold. (Perkins, 1987). A summary

of the conclusions of that paper are presented here, together with accounts of the features of the outer limits of the orebodies.

Summary of features indicative of epigenetic origin for lead-zinc orebodies

Characteristics of the lead-zinc mineralization as observed in hand specimen and microscopically which indicate a late replacement origin are summarized in Figure 12. This example shows three textural types of sphalerite. The first occurs as very fine (50-100µm) aggregates along the layering, with density variation occurring abruptly across sub-mm dolomite veins. The second occurs as much larger aggregates along bands with more coarsely crystalline dolomite, which still show relict layering, and the third is as aggregates along the cross-cutting dolomite veins themselves. These types would be regarded traditionally as 1) primary syngenetic/diagenetic sphalerite 2) recrystallization of primary sphalerite along bedding and 3) remobilization of sphalerite into cross-cutting veins during deformation. Examination of the distribution and textures of the sphalerite aggregates however, in particular the change in density across veins, the continuity of sphalerite aggregates from the bedded area into the walls of the veins, and the cross-cutting relationship of sphalerite across dolomite deformation lamellae, indicate only one generation of sphalerite which is later than the veins and alteration dolomite. An example of the continuity of galena and sphalerite from microveinlets to replacement of fine dolomite along bedding is shown in Figure 13.

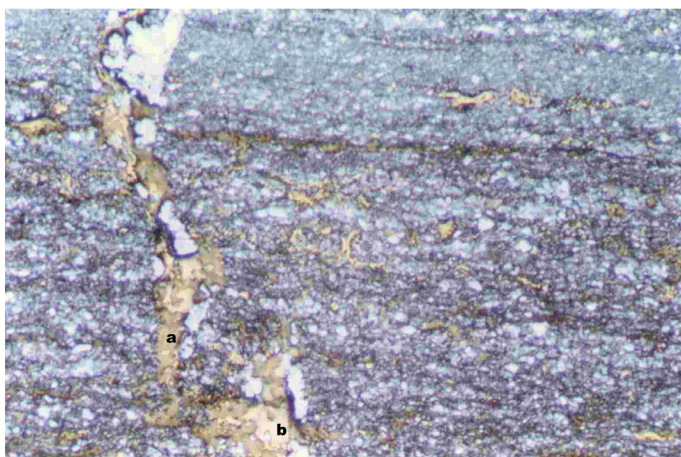
Figure 12. Different textural types of sphalerite in a single specimen.



Sphalerite aggregates along bedding extend along a 2.5mm wide zone with density highest at (A), lowest between the next two thin veins and intermediate above them. Sphalerite

along the central zone (B) is preferentially replacive after the clean white crystalline dolomite. In the zone on the left (with relict bedding) sphalerite (C) is interstitial to, and locally traverses, clean white "saddle dolomites" which overgrow inclusion-rich dolomite. In the veins eg (D), sphalerite aggregates are replacive after clean dolomites.. DDH K754 E. Decline #1, 15 Level 96.7m.

Figure 13. Sulphides along bedding and microveinlets.



Fine dolomite-quartz veinlet with sphalerite (a) and galena (b) extending from the veinlet into irregular replacive patches along bedding. Part reflected-part transmitted light. Blue colour the result of staining for ferroan dolomite. Field of view 2.2mm. 8 orebody 6910N, 2380 RL. Same sample as Perkins (1987) fig. 16a. and 18.

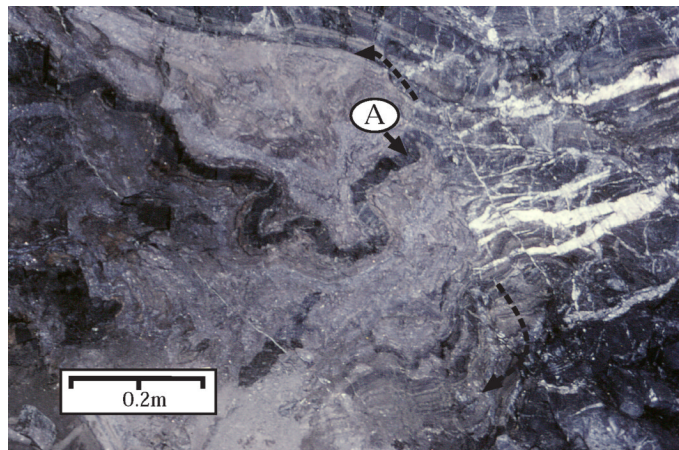
Fading out of the northern limits of lead-zinc orebodies

In syngenetic/early diagenetic models of lead-zinc ore formation it could be expected that ore grades would show a gradual diminution in a northerly direction towards the very low geochemistry in holes such as QZ10 (see Painter *et al.* fig. 1). In addition, enrichment would be expected in the Mount Isa Fold, if more ductile pre-deformation sulphides mobilized into fold hinges in the manner indicated for Hilton Mine by Valenta (1994). The observed lead and zinc grades, however, show a quite different relationship.

Ore grades in 7 orebody on 11 Level diminish abruptly from 7.0m. at 3.7% Pb and 8.2% Zn at 7270N to 500ppm Pb and 2400ppm Zn in the Mount Isa fold hinge only 45 metres north. The sharpness of this front can be as marked as that illustrated in Figure 14. Here a high-grade lead-zinc zone containing strongly folded non-laminated layers narrows down from >800mm to 460mm along a abrupt front with gently folded partially dolomitized layers containing two distinct generations of veins. The sub-horizontal veins are distinctly fibrous dolomite

veins and overprint the more carbonaceous veins showing dilation in a vertical direction. At the sulphide boundary galena-rich sulphides appear to have transgressed and replaced the fibrous dolomites over a short distance.

Figure 14. Abrupt termination of high-grade lead-zinc zone.



The high-grade zone on the left of the figure ends in a front shown by boundaries and arrows. Non-laminated siltstone layers (eg. A) can be traced into the veined area on the right which contains no visible galena and sphalerite. 7 orebody (below the F/W TMB) 9 Level 7070mN looking NE.

Similar relationships are observed in the vertical plane. At approximately 7200mN, a development face in 7 orebody (9C sublevel) contained 10% Zn across the face extending 0.4m below the 7 O/B F/W TMB. 12m directly above on 9E sublevel, the same zone extending 0.8m above the TMB contained no visible sphalerite. The dip was slightly shallower at the upper heading indicating proximity to the Mount Isa Fold. These observations indicate that the northern limits of lead-zinc orebodies are controlled by the change in orientation of bedding as the anticlinal hinge of the Mount Isa Fold is approached. It is indicative of local dilation along some bedding planes during shear associated with folding, allowed dolomitization and silicification along bedding which is subsequently replaced by sulphides.

FAQ-5. What observations and data are relevant to the relationship between fine-grained pyrite and the economic ores?

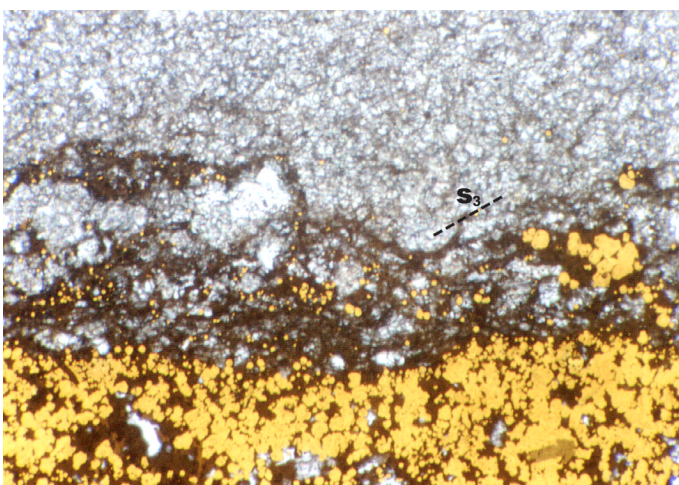
Painter *et al.* (1999) report observations and extensive sulphur isotope data on the fine-grained pyrite from the northern end of the lead-zinc system and extending for more than 11km northwards, as well as from south of the

mine. Some of these observations were regarded as supporting the interpretations of Perkins (1998) and some seemed to be inconsistent with them. Three of these aspects are discussed below.

Distribution of fine-grained pyrite

Differing interpretations exist on the extent to which concentrations of fine-grained pyrite are continuous along the same stratigraphy or transgress across it. The most detailed attempts to portray the distribution of fine-grained pyrite are by Perkins (1998) and Painter et al. (1999). The former focussed on the Mine area and the latter on the north end of the Mine and northwards. Both use a combination of their own observations and Mine records. Because of its fine grain size, (Figure 15) volumetric percentages of the earliest pyrite are notoriously difficult to estimate, with wide variation often showing between adjacent drill holes logged by different geologists. Added to this is the problem alluded to by Perkins et al 1998 (p. 1156) and Painter et al. (1999) of the difficulty of distinguishing between true fine-grained pyrite and "brassy pyrite" which is coarser-grained and far less continuous along bedding exposure. Within copper orebodies, there is the added complexity of allowing for the proportion of coarse-grained dolomite, quartz and chalcopyrite. Although relict bedding rich in fine-grained pyrite is common (Figure 16, Figure 17 and Figure 18) it may nonetheless constitute a minor percentage of the total rock volume.

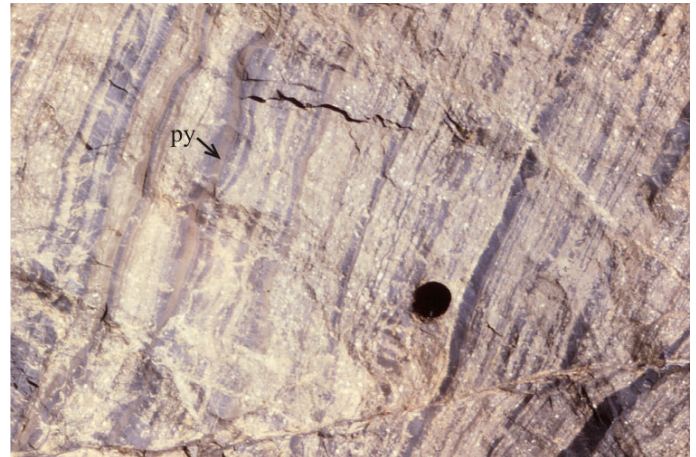
Figure 15. Fine-grained pyrite relationships.



Fine-grained pyrite along bedding (horizontal) and seams which anastomose between bedding and cleavage S₃. The grain size and variability of packing show how difficult it is to estimate pyrite percentage. Part transmitted/part reflected

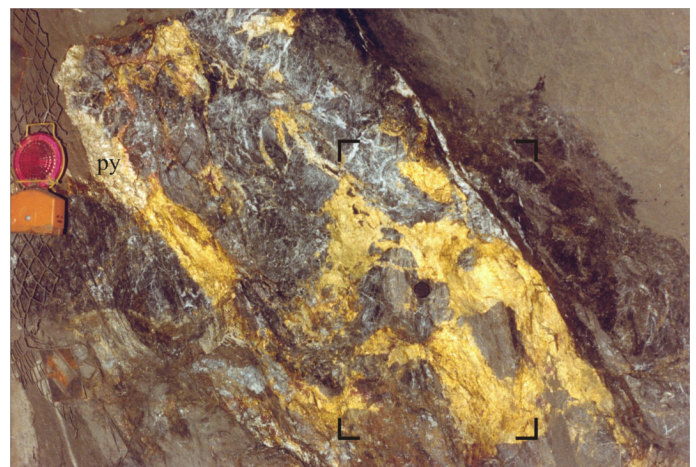
light. Field of view 0.6mm. 6 orebody 11 Level, 7172mN, 1652mE.

Figure 16. Fine-grained pyrite in the outer zone of silica-dolomite.



Sequence of dolomitized (whitish, banded) and silicified (dark grey) layers in the bedding-altered part of the silica-dolomite, showing layers rich in fine-grained pyrite (py, khaki). 400 orebody area 5/200 orebody stratigraphy 9 Level 5415mN. Looking north.

Figure 17. Fine-grained pyrite in high grade silicified zone of silica-dolomite.



Chalcopyrite-rich breccia with relict blocks containing a network of quartz veins after dolomite and some blocks with a high percentage of fine-grained pyrite along relict bedding. Looking south-west. Apart from an area of coarse-grained pyrite (py) the remaining near-massive sulphide in the matrix is chalcopyrite. The area of Figure 18 is shown. 18B sublevel 4802mN 1780mE.

Figure 18. Close-up of Figure 17.



Brown near-vertical layers in the block beneath the lens cap and the adjacent block are rich (~60%) in fine-grained pyrite.

Both authors agree that there is considerable continuity of fine-grained pyrite along bedding (see especially Painter *et al.* figures 7 and 8). Perkins (1998, fig. 6b) shows that within a sequence ranging in thickness from 35mm to 400mm (B sequence) fine-grained pyrite only occurs over a strike length of 2500m. In addition, there is no change in microfacies where pyrite is not deposited (Perkins, 1998, fig. 7). Painter *et al.* (1999) maintain that "local peaks in concentration of fine-grained pyrite are also evenly distributed throughout the formation" p. 893. Observation of fig. 7 of Painter *et al.* does appear to show a diminution of fine-grained pyrite concentration along strike from the Mine (K754) to QZ10. There is no evidence in their data to reflect the gross transgression of concentration across stratigraphy illustrated by Perkins

(1998, fig. 5b), which, despite the difficulties of estimation mentioned above, is so marked. There is not sufficient "brassy pyrite" for the Mine pyrite transgression to be explained by this overprint alone, as suggested by Painter *et al.* p. 909. In fact, to the north of Mine the 8 orebody sequence in QZ10 contains significant pyrite while the overlying 7 orebody sequence is almost devoid of it. This is the reverse of the trend expected if the transgression to the hangingwall were still in evidence at this northing. In summary, it seems more likely that the transgression occurs in the mine where it is related to the Mount Isa Fold but not to the north of it in the area studied by Painter *et al.* (1999).

Timing of fine-grained pyrite deposition

This remains a debated issue. It is agreed (eg. Grondjic and Schouten, 1937; Perkins, 1997; Painter *et al.*, 1999) that fine-grained pyrite everywhere precedes the deposition of sphalerite, galena, and chalcopyrite. Perkins (1998) presented evidence for fine-grained pyrite deposition subsequent to the S_3 cleavage and Painter *et al.* (1999) argued for diagenetic deposition. Although both authors agree that fine-grained pyrite has precipitated primarily in the finely laminated siltstone sequences, there are differences in interpretation of these sequences. Painter *et al.* base their sedimentological interpretation on the detailed work of Neudert (1983), where the laminated sequences are regarded as being derived from the compaction of the cross-laminated siltstone bases of the graded beds of the rythmite facies. While not being a sedimentological study, Perkins (1997, fig. 4) illustrates correlation of individual laminae over 3 km which would appear to indicate that each lamination was deposited sequentially, and would preclude the whole package being the basal part of a single bed. This publication was not referred to by Painter *et al.* (1999).

There are significant differences in interpretation of the timing of fine-grained pyrite deposition between these two papers. Painter *et al.* (their fig. 10) note that fine-grained pyrite appears to overprint the carbonaceous seams in their "laminated siltstone portion of a rythmite facies bed" and larger scale dissolution seams (their fig. 11), indicating that this pyrite "must have occurred either during, or later than, the development of diagenetic dissolution textures in the Urquhart Shale". In terms of an earliest time limit for deposition, this accords with Perkins (1998). However, Swager (1985) and Perkins (1997)

argue that carbonaceous seams parallel to bedding are enhanced during one or more periods of deformation prior to the main episode of folding in the Mine. If this is so, pyrite overprinting such seams is necessarily post-diagenetic.

Observations of Painter *et al.*, (1999) and Perkins (1998) appear to be inconsistent with respect to the relationship between fine-grained pyrite and cross-cutting cleavage seams. Figures 8 and 9 of Perkins (1998) illustrate concentrations of fine-grained pyrite along, and also transecting, cross-cutting cleavage (S_3) seams, and individual zoned pyrites overgrowing narrow seams. In contrast, Painter *et al.* (1999, fig. 12) show a series of four wavy bedding-parallel laminae containing abundant fine-grained pyrite. Interstitial mudstones show a well-developed cross-cutting foliation (probably S_3). In the text, this foliation is referred to as "carbonaceous" (p.895), but appears in the photograph to be more planar and penetrative than the commonly anastomosing carbonaceous S_3 cleavage. If this cleavage is not carbonaceous, then this could explain the lack of fine-grained pyrite along it, and need not necessarily mean that the pyrite is earlier than the cleavage. Perkins' evidence of post- S_3 deposition from a series of examples have not been refuted, however the example of Painter *et al.* requires re-examination.

Sources of metals and sulphur

According to Painter *et al.* (1999) all components for the formation of fine-grained pyrite were endogenic to the system with sulphur derived from sulphate evaporites and iron from the carbonates. This is in contrast to Perkins (1997, 1998) where it was argued that local sulphates were replaced by dolomites and quartz before the formation of fine-grained pyrite at a late stage in the deformation history. In this model, both iron and sulphur was introduced. Examples such as Figure 16, Figure 17, and Figure 18 indicate that the sulphur from fine-grained pyrite was not a sulphur source for chalcopyrite deposition. Both studies support a model of sulphate reduction at the site of precipitation, although that of Perkins (1998) does not countenance a bacteriogenic reaction. Painter *et al.* (1999) provide detailed analysis of the sulphur isotopes of all major sulphide species, and conclude that the Pb-Zn and Cu orebodies probably shared a common sulphur source. They envisaged either a cogenetic model similar to that of Perkins (1997) or a two-stage model. Their synoptic diagram (fig. 20) with lead-zinc orebodies formed while bedding was still horizontal suggests they favoured the latter alternative.

References

- Croxford, N. J. W. 1962. The mineralogy of the no. 7 lead-zinc orebody, Mount Isa, and its interpretation. Unpubl. PhD thesis, Univ. New England, Armidale, 284p.
- Croxford, N. J. W. 1964. Origin and significance of volcanic potash-rich rocks from Mount Isa. Transactions of the Institute of Metallurgy. 74, 34-43.
- Davis, T. P. 2004. Mine-scale structural controls on the Mount Isa Zn-Pb-Ag and Cu orebodies. Economic Geology. 99, 543-559. 10.2113/99.3.543
- Grondijis, M.F., and Schouten. C. 1937. A study of the Mount Isa ores. Economic Geology. 32, 407-450. 10.2113/gsecongeo.32.4.407
- Heinrich, C. A., Andrew, A. S., Wilkins, R. W. T., and Patterson, D. J. 1989. A fluid inclusion and stable isotope study of synmetamorphic copper ore formation at Mount Isa, Australia. Economic Geology. 84, 529-550. 10.2113/gsecongeo.84.3.529
- Painter, M. G. M., Golding, S. D., Hannan, K.W., and Neudert, M. K. 1999. Sedimentologic, petrographic, and sulfur isotope constraints on fine-grained pyrite formation at Mount Isa Mine and environs. Economic Geology. 94, 883-912. 10.2113/gsecongeo.94.6.883
- Neudert, M. K. 1983. A depositional model for the Upper Mount Isa Group and implications for ore formation. PhD thesis. Australian National University. Sedcon Publications.
- Perkins, W. G. 1984. Mount Isa silica-dolomite and copper orebodies: The result of a syntectonic hydrothermal alteration system. Economic Geology. 79, 601-637. 10.2113/gsecongeo.79.4.601
- Perkins, W. G. 1997. Mount Isa lead-zinc orebodies: Replacement lodes in a zoned syndeformational copper-lead-zinc system? Ore Geology Reviews. 12, 61-110. 10.1016/S0169-1368(97)00004-8
- Perkins, W. G. 1998. Timing of formation of Proterozoic stratiform fine-grained pyrite: Post-diagenetic cleavage replacement? Economic Geology. 93, 1153-1164. 10.2113/gsecongeo.93.8.1153
- Perkins, W. G., and Bell T. H., 1998, Stratiform replacement lead-zinc deposits: A comparison between Mount Isa, Hilton, and McArthur River. Economic Geology, 93, 1190-1212. 10.2113/gsecongeo.93.8.1190
- Proffett, J. M. 1990. Some new observations on the geologic structure south-west of Mount Isa. Mount Isa Inlier Geology Conference, (abs). Victorian Institute of Earth and Planetary Sciences, Monash University, 29-31.
- Swager, C. P. 1985. Syndeformational carbonate-replacement model for the copper mineralization at Mount Isa, northwest Queensland: A microstructural study. Economic Geology. 80, 107-125. 10.2113/gsecongeo.80.1.107
- Valenta, R. K. 1994. Deformation of host rocks and stratiform mineralization in the Hilton Mine area, Mount Isa. Australian Journal of Earth Sciences. 41, 429-443. 10.1080/08120099408728153
- Waring, C. L. 1990. Genesis of the Mount Isa copper ore system. Unpublished PhD thesis, Monash University. Melbourne. 303p